Eur. Phys. J. B (2013) 86: 263
DOI: 10.1140/epjb/e2013-31065-9

THE EUROPEAN PHYSICAL JOURNAL B

Regular Article

The rhythm of coupled metronomes

Sz. Boda, Z. Néda[a], B. Tyukodi, and A. Tunyagi

Babeş-Bolyai University, Department of Physics, str. Kogălniceanu nr. 1, 400084 Cluj-Napoca, Romania

Received 22 November 2012 / Received in final form 28 March 2013
Published online 12 June 2013 –

Abstract. Spontaneous synchronization of an ensemble of metronomes placed on a freely rotating platform is studied experimentally and by computer simulations. A striking in-phase synchronization is observed when the metronomes' beat frequencies are fixed above a critical limit. Increasing the number of metronomes placed on the disk leads to an observable decrease in the level of the emerging synchronization. A realistic model with experimentally determined parameters is considered in order to understand the observed results. The conditions favoring the emergence of synchronization are investigated. It is shown that the experimentally observed trends can be reproduced by assuming a finite spread in the metronomes' natural frequencies. In the limit of large numbers of metronomes, we show that synchronization emerges only above a critical beat frequency value.

1 Introduction

Spontaneous synchronization of coupled non-identical oscillators is a well-known form of collective behavior [1–3]. The problem has been intensively studied since Huygens. If the legend is true, presumably he was the first one who noticed and reported the synchronized swinging of pendulum clocks. By simple experiments he found that the synchronized state is a stable limit cycle of the system, because even after perturbing the system, the pendulums came back to this dynamic state. Originally, Huygens thought that this *"odd kind of sympathy"*, as he named it, occurs due to shared air currents between the pendulums. He performed several tests to confirm this idea. His experimental setup was really simple, with two pendulum clocks hung from a common suspension beam which was placed between two chairs [3]. After performing some additional tests, Huygens observed a stable and reproducible anti-phase synchronization, and attributed this to imperceptible vibrations in the suspension beam. He summarized his observations in a letter to the Royal Society of London [4], and launched the study of synchronization phenomena and coupled oscillators.

Recent studies have aimed at reconsidering various forms of Huygens' two pendulum-clock experiment as well as realistically modelling the system. Bennet et al. [5] investigated the same two pendulum-clock system as Huygens did and came to the conclusion that several types of collective dynamics are observable as a function of the system's parameters. For strong coupling, a "beat death" phenomenon usually occurs where one pendulum oscillates and the other does not. For weak coupling, synchronization does not occur, and a quasi-periodic oscillation is observed. There is, however, an intermediate coupling strength interval where the anti-phase synchronization observed by Huygens appears. Hence, Huygens had some luck with his setup as the coupling was just in the right interval: strong enough to cause synchronization, but also weak enough to avoid the "beat death" phenomenon.

Dilao [6] came to the conclusion that the periods of two synchronized nonlinear oscillators (pendulum clocks) differ from the natural frequencies of the oscillators. Kumon et al. [7] have studied a similar system consisting of two pendulums, one of them having an excitation mechanism, and the two pendulums being coupled by a weak spring. Fradkov and Andrievsky [8] developed a model for such a system, and obtained from numerical solutions that both in- and anti-phase synchronizations are possible, depending on the initial conditions.

Czolczynski et al. [9] revisited Huygens' original experiment and found that the anti-phase synchronization usually emerges, although in rare cases in-phase synchronization is also possible. They also developed a more realistic model for this experiment [10].

Pantaleone [11] considered a similar system, but he used metronomes placed on a freely moving base (suspended on two cylinders) instead of pendulum clocks. He modeled the metronomes as van der Pol oscillators [12] and came to the conclusion that anti-phase synchronization occurs in some rare cases only. He proposed this setup as an easy classroom demonstration for the Kuramoto model [13] and extended the study for larger systems containing up to seven globally coupled metronomes. He also made quantitative investigations by tracking the motion of the metronomes' pendulum by acoustically registering the ticks with a microphone. Ulrichs et al. [14] examined the case when the number of metronomes was even larger.

[a] e-mail: zneda@phys.ubbcluj.ro

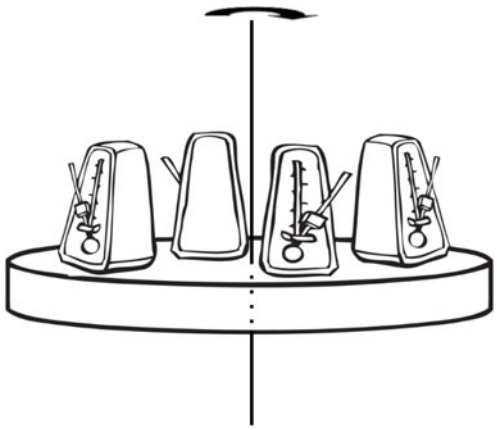

Fig. 1. Schematic view of the experimental setup: metronomes are placed on the perimeter of a disk that can rotate around a vertical axes.

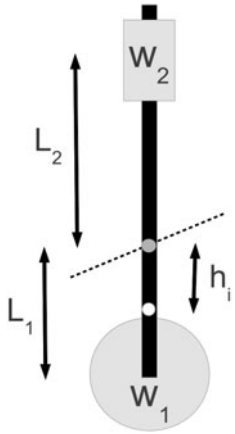

Fig. 2. Schematic view of the metronomes' bob. The dotted line denotes the horizontal suspension axis, and the white dot illustrates the center of mass.

The present state of this quite old field of physics was recently reviewed by Kapitaniak et al. [15].

Our work is intended to continue this line of studies showing that it is still possible to find interesting aspects of this quite old problem in physics. In contrast to previous works, we consider an ensemble of metronomes arranged symmetrically on the perimeter of a freely rotating disk, as illustrated in Figure 1. The free rotation of the disk acts as a coupling mechanism between the metronomes and, for high enough ticking frequencies, synchronization emerges. Our aim here is to investigate the conditions favoring such spontaneous synchronization by using a realistic model and model parameters. In order to achieve our task, we first study the dynamics of the system by well-controlled experiments. Contrary to earlier studies that investigated only the final stable dynamic state of the system, here we also consider and describe the transient dynamics leading to synchronization. The synchronization level is quantified and measured. This is achieved by using an optical phase-detection mechanism for each metronome separately. We then construct a realistic model for the system and its modeling power is proved by comparing its results with the experimental ones. We discuss the reasons behind the fact that only in-phase synchronization is observed in our experiments. Finally, the model is used to investigate the emergence of synchronization in large ensembles of coupled metronomes.

2 Experimental setup

The experimental setup is sketched in Figure 1. The main units are the metronomes (Figs. 1 and 3a), which are devices that produce regular, metrical beats. They were patented by Johann Maelzel in 1815 as a timekeeping tool for musicians [16]. The oscillating element of the metronome is a physical pendulum, which consists of a rod with two weights on it (Fig. 2): a fixed one at the lower end of the rod, whose mass is denoted by W_1, and a movable one, W_2, attached to the upper part of the rod. In general, $W_1 > W_2$ and the rod is suspended on a horizontal axis between the two weights in a stable manner, so that the center of mass lies below the suspension axes.

By sliding the W_2 weight along the rod, the oscillation frequency can be tuned. There are several marked places on the rod where the W_2 weight has a stable position, yielding standard ticking frequencies for the metronome. These ω_0 frequencies are marked on the metronome in units of beats per minute (BPM).

Another key part of the metronomes is the excitation mechanism, which compensates for the energy lost to friction. This mechanism gives additional momentum to the physical pendulum in the form of pulses delivered at a given phase of the oscillation period. For a more detailed analysis of this excitation mechanism we recommend the work of Czolczynski et al. [10].

For the experiments, we used the commercially available Thomann 330 metronomes (Fig. 3a). From the 10 metronomes we had bought, the 7 with the most similar frequencies were selected. Naturally, since there are no two identical units, we have to deal with a non-zero standard deviation of the natural frequencies in experiments

In order to globally couple the metronomes, we placed them on a disk shaped platform which could rotate with a very little friction around a vertical axis, as is sketched in Figure 1 and illustrated in the photo in Figure 3a.

In order to monitor the dynamics of all metronomes separately, photo-cell detectors (Fig. 3b) were mounted on them. These detectors were commercial ones (Kingbright KTIR 0611 S), and contained a light emitting diode and a photo-transistor. They were mounted on the bottom of the metronomes.

The wires starting from each metronome (seen in Fig. 3) connect the photo-cell to a circuit board, allowing data collection through the USB port of a computer. The data was collected using a free, open-source program, called *MINICOM*. [17]. The data was saved in log files, and could be processed in real-time. It was possible to simultaneously follow the states of up to 8 metronomes. The circuit board only sent data when there was a change in

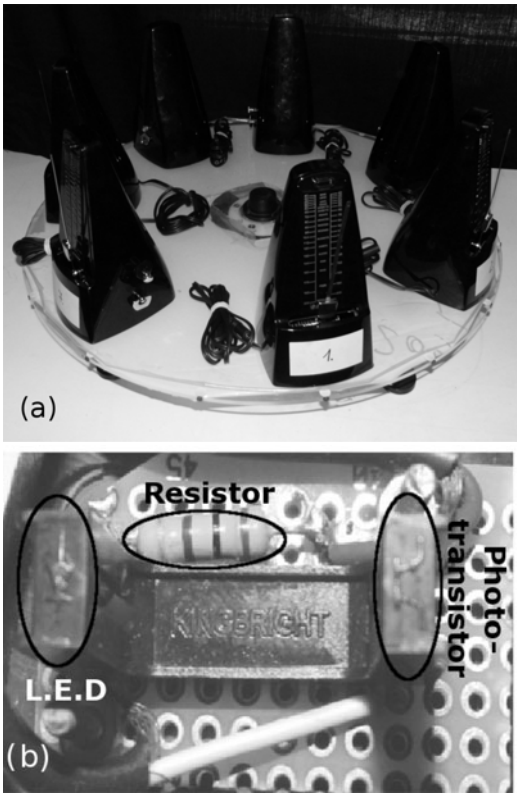

Fig. 3. (a) The experimental setup, with the metronomes placed on the platform and the wiring that carries information on the metronomes' phases. (b) One of the light-gates (Kingbright KTIR 0611 S), composed of an infrared LED and a photo-transistor.

the signal from the photo-cell system (i.e. a metronome's bob passed the light-gate). At that point, it would record a string such as $0-0-1-1-0-1-0$ 1450, where the first 7 numbers characterize the metronome bob's position relative to the photo-cell (whether the gate is open or closed) and the eighth number is the time, where one time unit corresponds to 64 microseconds. Since we are interested in the dynamics of this system from the perspective of synchronization, we computed the classical order parameter, r, of the Kuramoto model [13] in our numerical evaluations:

$$r\exp(i\phi) = \frac{1}{N}\sum_j \exp(i\theta_j). \quad (1)$$

Here, ϕ is the average phase of the whole ensemble, θ_j is the phase of the jth metronome, N is the number of metronomes, and i is the imaginary unit.

The recorded data only tell us the exact moment at which the metronome's bob passes through the light-gate, so some additional steps are needed in order to get the phases θ_j of all metronomes and to compute the Kuramoto order-parameter for a given moment in time. In order to achieve this, we first excluded from the data those time-moments when the metronome's bob passed through the light-gate for the second time in a period, and after that we retained the pass-times corresponding to a given directional motion only. With this "cleaned data", we calculated the period of each cycle and interpolated this time-interval for the θ_j phases (between 0 and 2π, corresponding to the state of a Kuramoto rotator) assuming a uniform angular-velocity. This way, the phase θ_j of each metronome (considered here as a rotator) could be uniquely determined at each moment in time, and the Kuramoto order parameter (1) could be computed.

Table 1. Standard deviation of the seven metronomes used for different nominal frequencies.

ω_0 (BPM)	160	168	176	184	192	208
σ (BPM $\times 10^{-7}$)	8.4	7.9	7.8	9.8	8.5	8.7

Before starting the experiments, we monitored each metronome separately and recorded their exact frequency, ω_i, for all the standardly marked rhythms. These frequencies had a small, but finite fluctuation around the nominal frequency, ω_0. We have selected those 7 metronomes that had their ω_i standard frequencies relatively close to each other, and precisely measured these values. From these values the standard deviation, σ, of the used metronomes' natural frequencies could be determined (Tab. 1).

3 Experimental results

As already described in the introductory section, the metmetronomes oscillate with different natural frequencies, depending on the position of the adjustable weight on the metronomes' rod. For our experiments we have used the standard frequencies marked on the metronome. These frequencies are given in BPM units.

Before discussing the experimental results in detail, we have to emphasize that, independently of the chosen initial condition, only in-phase synchronization of the metronomes was observed. The reasons for this will be given in a separate section (Sect. 6).

In the very first experiments, we were studying how the chosen frequency influences the detected synchronization level. We fixed all the metronomes' frequencies on the same marked ω_0 value and placed them symmetrically on the perimeter of the rotating platform as indicated in Figure 3a. In reality, of course, this does not mean that their frequencies were exactly the same since no two macroscopic physical systems can be exactly identical. We initialized the system by starting the metronomes randomly, and let the system composed of the metronomes and platform evolve freely.

For each considered frequency value we made 10 measurements, collecting data for 10 min. The dynamics of the computed Kuramoto order parameter averaged across the 10 independent experiments are presented in Figure 4a.

The results suggest that the obtained degree of synchronization increases as the metronomes' natural frequencies increase. The standard deviations of the natural frequencies of the independent oscillators are indicated in Table 1.

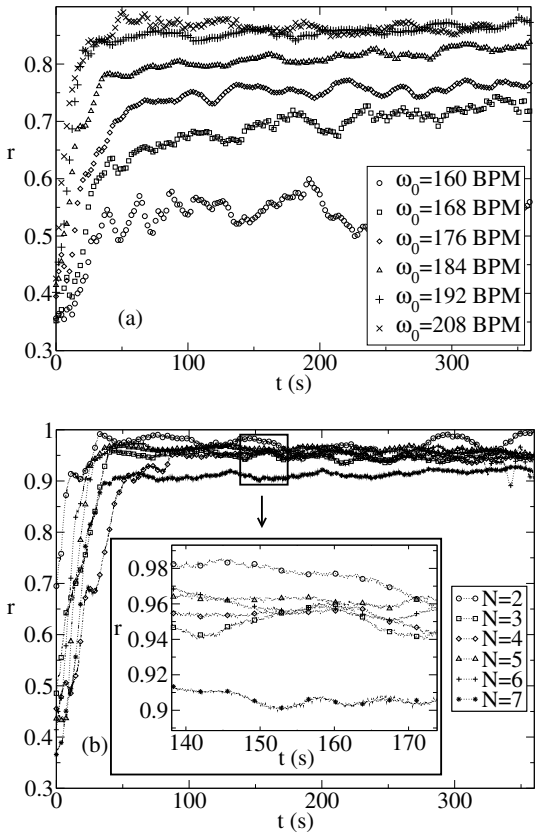

Fig. 4. Dynamics of the order parameter for different natural frequencies and numbers of metronomes. (a) Results for seven metronomes, different curves corresponding to different frequencies as indicated in the legends. (b) Results are for the fixed frequency ($\omega_0 = 192$ BPM) and different numbers of metronomes as indicated in the legend. On both graphs, the results are averaged across 10 independent measurements.

Since there is no clear trend in this data as a function of ω_0, the obtained result suggests that the observed effect is not due to a decreasing trend in the metronomes' standard deviation. We have also found that, for the standard metronome frequencies below 160 BPM, the system did not synchronize. It is interesting to note, however, that if one inspects visually or auditorily the system, one would observe no synchronization for frequencies already below 184 BPM. This means that we are not suited to detect partial synchronization with an order parameter below $r = 0.75$.

In a second experiment, we were investigating the influence of the number of metronomes on the synchronization level. In order to study this, we fixed the metronomes at the same frequency ($\omega_0 = 192$ BPM) and repeated the previous experiment with increasing numbers of metronomes placed on the rotating platform.

Again, we performed 10 measurements for each configuration so as to obtain accurate results and averaged the observed order parameter. The averaged results are presented in Figure 4b.

Although the standard deviation of the metronomes' natural frequencies (Tab. 2) does not present a clear trend as a function of the number of metronomes, N, we see a clear trend in the detected synchronization level: increasing the number of metronomes will result in a decrease in the synchronization level.

Table 2. Standard deviation of the metronomes' natural frequencies for different numbers of metronomes on the rotating platform ($\omega_0 = 192$ BPM).

N	2	3	4	5	6	7
σ (BPM $\times 10^{-7}$)	5.1	8.1	7.5	7.1	6.7	8.5

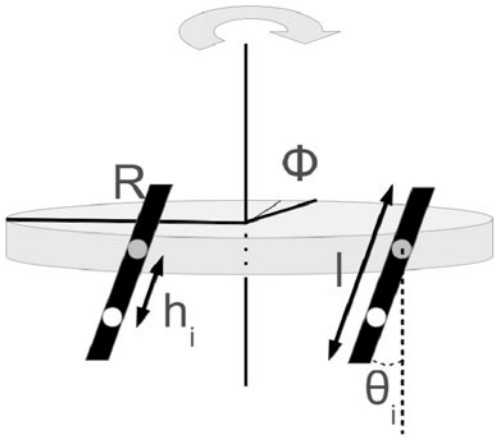

Fig. 5. Schematic view and notations for the considered mechanical model. The white dots denote the center of mass of the physical pendulums and the gray dots are the suspension axes.

4 Theoretical model

Inspired by the model described in reference [10], it is possible to consider a simple mechanical model for the system investigated here. The model is composed of a rotating platform and physical pendulums attached to its perimeter, as is sketched in Figure 5.

The Lagrange function of such a system is written as:

$$L = \frac{J}{2}\dot{\phi}^2 + \sum_{i=1}^{N}\frac{J_i\omega_i^2}{2} + \sum_{i=1}^{N}\frac{m_i}{2}\left\{\left[\frac{d}{dt}\left(x_i + h_i\sin\theta_i\right)\right]^2 + \left[\frac{d}{dt}\left(h_i\cos\theta_i\right)\right]^2\right\} - \sum_{i=1}^{N} m_i g h_i(1-\cos\theta_i). \quad (2)$$

The first term is the kinetic energy of the platform, the second is the kinetic energy due to the rotation of the pendulum around its center of mass, the third one is the kinetic energy of the pendulum's center of mass, and the last term is the potential energy of the pendulum. In the Lagrangian we have used the following notations: the index i denotes the pendulums, J is the moment of inertia of the platform with the metronomes on it – taken relative to the vertical rotation axes, ϕ is the angular displacement of the platform, m_i is the total mass of the pendulum

($m_i \approx W_1^{(i)} + W_2^{(i)}$, neglecting the mass of the rod), h_i is the distance between the center of mass and the suspension point of the pendulum, x_i is the horizontal displacement of the suspension point of the pendulums due to the rotation of the platform, θ_i is the displacement of the ith pendulum's center of mass, in radians, J_i is the moment of inertia of the pendulum relative to its center of mass and ω_i is the angular velocity of the rotation of the pendulum relative to its center of mass. It is easy to see that $x_i = R\dot{\phi}$ and $\omega_i = \dot{\theta}_i$. Assuming now that the mass of all the weights suspended on the metronomes' bobs are the same ($W_1^{(i)} = w_1$, $W_2^{(i)} = w_2$, and consequently $m_i = m$), and disregarding the $m_i g h_i$ constant terms, one obtains:

$$L' = \left(\frac{J + NmR^2}{2}\right)\dot{\phi}^2 + \sum_i \left(\frac{mh_i^2}{2} + \frac{J_i}{2}\right)\dot{\theta}_i^2 + mR\dot{\phi}\sum_i h_i \cos\theta_i \cdot \dot{\theta}_i + mg\sum_i h_i \cos\theta_i. \quad (3)$$

The Euler-Lagrange equations of motion yield:

$$\left(J + NmR^2\right)\ddot{\phi} + mR\sum_i h_i\left[\ddot{\theta}_i \cos\theta_i - \dot{\theta}_i^2 \sin\theta_i\right] = 0, \quad (4)$$

$$\left[mh_i^2 + J_i\right]\ddot{\theta}_i + mR\ddot{\phi}h_i \cos\theta_i + mgh_i \sin\theta_i = 0. \quad (5)$$

The above equations of motion are for a Hamiltonian system where there is no damping (no friction) and no driving (excitation). Friction and excitation from the metronomes' driving mechanism has to be taken into account with some extra terms. The system of equations of motion may be written as:

$$(J + NmR^2)\ddot{\phi} + mR\sum_i h_i\left[\ddot{\theta}_i \cos\theta_i - \dot{\theta}_i^2 \sin\theta_i\right] + c_\phi\dot{\phi} + \sum_i \mathbb{M}_i = 0 \quad (6)$$

$$\left[mh_i^2 + J_i\right]\ddot{\theta}_i + mR\ddot{\phi}h_i \cos\theta_i + mgh_i \sin\theta_i + c_\theta\dot{\theta}_i = \mathbb{M}_i, \quad (7)$$

where c_ϕ and c_θ are coefficients characterizing the friction in the rotation of the platform and pendulums, and $\mathbb{M}_i$ are some instantaneous excitation terms defined as:

$$\mathbb{M}_i = M\delta(\theta_i)\dot{\theta}_i, \quad (8)$$

where δ denotes the Dirac function and M is a fixed parameter characterizing the driving mechanism of the metronomes. The choice of the form for $\mathbb{M}_i$ in equation (8) means that excitations are given only when the metronome's bob passes the $\theta = 0$ position. The term $\dot{\theta}$ is needed in order to ensure a constant momentum input, independently of the metronomes' amplitude. It also ensures that the excitation is given in the correct direction (the direction of motion). It is easy to see that the total momentum transferred, $\mathbb{M}_{trans}$, to the metronomes in a half period ($T/2$) is always M:

$$\mathbb{M}_{trans} = \int_t^{t+T/2} M\delta(\theta_i)\dot{\theta}_i dt = \int_{-\theta_{\max}}^{\theta_{\max}} M\delta(\theta_i)d\theta_i = M.$$

This driving will be implemented in the numerical solution as:

$$\mathbb{M}_i = \begin{cases} M/dt & \text{if } \theta_i(t-dt) < 0 \text{ and } \theta_i(t) > 0 \\ -M/dt & \text{if } \theta_i(t-dt) > 0 \text{ and } \theta_i(t) < 0 \\ 0 & \text{in any other case} \end{cases}$$

where dt is the time-step in the numerical integration of the equations of motion. Clearly, this driving leads to the same total momentum transfer M as the one defined by equation (8).

The coupled system of equations (6) and (7) can be written in a form more suitable for numerical integration:

$$\ddot{\phi} = \frac{mR\sum_i h_i\dot{\theta}_i^2 \sin\theta_i - c_\phi\dot{\phi} - \sum_i \mathbb{M}_i + A + B - C}{D}, \quad (9)$$

$$\ddot{\theta}_i = \frac{\mathbb{M}_i - mR\ddot{\phi}h_i \cos\theta_i - mgh_i \sin\theta_i - c_\theta\dot{\theta}_i}{mh_i^2 + J_i}, \quad (10)$$

where

$$A = m^2 gR\sum_i \frac{h_i^2 \sin\theta_i \cos\theta_i}{mh_i^2 + J_i},$$

$$B = mRc_\theta\sum_i \frac{h_i\dot{\theta}_i \cos\theta_i}{mh_i^2 + J_i},$$

$$C = mR\sum_i \frac{h_i M_i \cos\theta_i}{mh_i^2 + J_i},$$

$$D = \left(J + NmR^2 - m^2R^2\sum_i \frac{h_i^2 \cos^2\theta_i}{mh_i^2 + J_i}\right).$$

Now taking into account that the metronomes' bobs have the form sketched in Figure 2b and the L_1 distances are fixed and assumed to be identical for all the metronomes, the h_i and J_i terms of the physical pendulums in our model will be calculated as:

$$h_i = \frac{1}{w_1 + w_2}\left(w_1 L_1 - w_2 L_2^{(i)}\right) \quad (11)$$

$$J_i = w_1 L_1^2 + w_2\left(L_2^{(i)}\right)^2. \quad (12)$$

5 Realistic model parameters

The parameters were chosen following the experimental device: $w_1 = 0.025$ kg, $w_2 = 0.0069$ kg, $L_1 = 0.0358$ m, $L_2 \in [0.019, 0.049]$ m depending on the chosen natural frequency, $R = 0.27$ m and $J \in [0.0729, 0.25515]$ kg m^2 depending on the number of metronomes placed on the platform.

The damping and excitation coefficients were estimated as follows. For the estimation of c_θ, a single metronome on a rigid support was considered. Switching off the excitation mechanism, a quasi-harmonic damped oscillation of the metronome took place. The exponential decay of its amplitude as a function of time uniquely

defines the damping coefficient, hence a simple fit of the amplitude as a function of time allowed the determination of c_θ. Switching the excitation mechanism on lead to a steady-state oscillation regime with constant amplitude. Since c_θ has already been measured, this amplitude value is defined by the excitation coefficient M. Solving equations (6) and (7) for a single metronome and tuning it until the same steady-state amplitude is obtained as in experiments makes the estimation of M possible. Now that both c_θ and M are known, the following scenario is considered: all the metronomes are placed on the platform and synchronization is reached. Then the platform has a constant-amplitude oscillatory motion. In order to determine c_ϕ, its value is tuned while solving equations (6) and (7) until the same amplitude of the disk's oscillations is obtained as in the experiments. This way, all the parameters in the model can be related to the experimental quantities. Using the method defined above, we estimated the following parameter values: $c_\theta = 0.00005$ kg m^2/s, $c_\phi = 0.00001$ kg m^2/s and $M = 0.0006$ Nm/s.

6 In-phase synchronization versus anti-phase synchronization of two metronomes

As described in the introductory section, many previous works have reported a stable anti-synchronized state in the case of two coupled oscillators [5,8,9]. Due to the fact that no such stable phase was observed in our experiments (independently of the starting conditions), we feel that investigating this issue is important. Starting from our theoretical model described in Section 4, we will show that the in-phase synchronization is favored whenever there are large enough equilibrated damping and driving forces acting on the metronomes.

First, let us investigate the case without any damping and with no driving forces. The equations of motion for such a system are given by equations (4) and (5). Considering the case of two identical metronomes ($N = 2$) with small-angle deviations ($\theta_{1,2}^{\max} \ll \pi/2$), we investigate the synchronization properties of such a system. The synchronization level will be studied here by an appropriately chosen order parameter for two metronomes, z, that indicates whether we have in-phase or anti-phase synchronization. Although we could have used the Kuramoto order parameter for this purpose, we decided to introduce a new, more suitable order parameter. Note that this new order parameter is only useful for small ensembles, because its calculation would be very time consuming for large systems. In order to introduce a proper order parameter, let us consider the dynamics of two metronomes as a function of time by plotting $\theta_{1,2}(t)$ (Fig. 6). Let us denote the time-moments where metronome i reaches a local minimum and maximum θ_1 values by $t_i^{\min}$ and $t_i^{\max}$, respectively. We denote the time-moments where metronome 2 has local maximum θ_2 values by $T_j^{\max}$. With these notations, we define two time-like quantities that characterize the average time-interval of the maximum position of $\theta_2(t)$ relative to the maximum and minimum positions of $\theta_1(t)$,

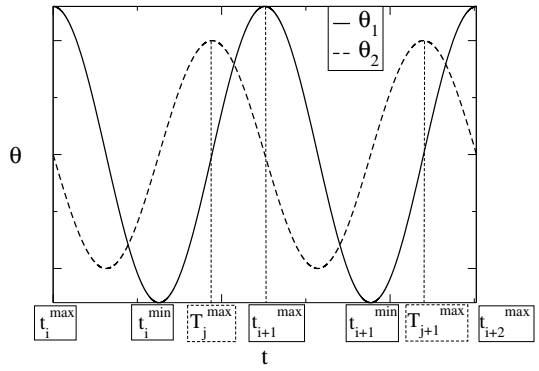

Fig. 6. Dynamics of two metronomes as a function of time, and the quantities used for defining the z order parameter.

respectively:

$$t_1 = \left\langle \min_{\{i\}} \left\{ \left| t_i^{\max} - T_j^{\max} \right| \right\} \right\rangle_j , \tag{13}$$

$$t_2 = \left\langle \min_{\{i\}} \left\{ \left| t_i^{\min} - T_j^{\max} \right| \right\} \right\rangle_j . \tag{14}$$

In the above equations the averages are considered over all j maximum positions of $\theta_2(t)$, and the "min" notation refers to the minimal value of the quantity in the brackets. Now, the z order parameter is defined as:

$$z = \frac{t_2 - t_1}{t_2 + t_1}. \tag{15}$$

It is easy to see that z is bounded between -1 and 1. For totally in-phase synchronized dynamics we have $t_1 = 0$, leading to $z = 1$. For totally anti-phase synchronized dynamics $t_2 = 0$, and we get $z = -1$. Negative z values suggest a dynamic where the anti-phase synchronized states are dominant, positive z values suggest a dynamic with more pronounced in-phase synchronized states.

The z order parameter was estimated numerically for different initial conditions. A velocity Verlet-type algorithm was used, and simulations were performed up to a $t = 4000$ s time interval, with a $dt = 0.01$ s time-step.

Initially the deviation angle of the first metronome was chosen as $\theta_1(0) = \theta_{\max} = 0.1$ rad and $\theta_2(0)$ was chosen in the interval $[-0.1, 0.1]$ rad, leading to various initial phase-differences between them. The computed z values as a function of $\theta_2(0)$ are plotted in Figure 7.

The above results suggest that for the friction-free and undriven case (Fig. 7), synchronization and phase-locking of coupled identical metronomes are possible only if they start either in completely in-phase or completely anti-phase configurations. Depending on how the phases are initialized, the ticking dynamics statistically resemble either the in-phase or the anti-phase states, but no phase-locking or synchronization is observable. Starting from an arbitrary initial condition a complete in-phase or anti-phase synchronization is possible only if there is dissipation and driving. For small dissipation and driving values both the in-phase and anti-phase synchronization are possible, as the results obtained for $M = 6 \times 10^{-5}$ Nm/s

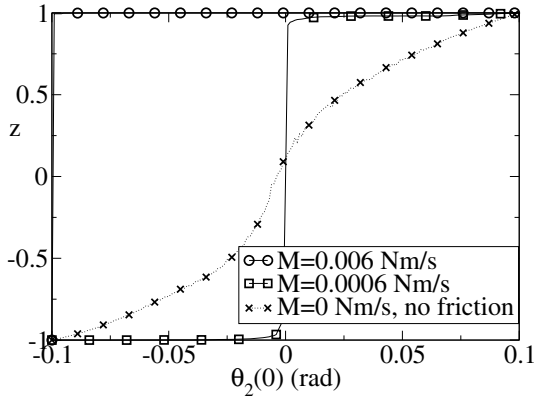

Fig. 7. The z order parameter as function of the initial phase $\theta_2(0)$. The results obtained without damping ($c_\theta = 0$, $c_\phi = 0$) and driving ($M = 0$) indicate that phase-locking and complete synchronization is possible only if the system starts from such a situation. For small damping and driving values ($M = 6 \times 10^{-5}$ Nm/s), both in-phase and anti-phase synchronization is possible. For large driving intensities ($M = 6 \times 10^{-4}$ Nm/s), only the in-phase synchronization is stable. The later is the realistic parameter for the experimental metronome setup.

suggest. In this limit in-phase synchronization will emerge if the initial phases are closer to such a situation. Alternatively, if the initial conditions resemble the anti-phase configuration, a stable anti-phase synchronization emerges. For higher dissipation and driving values (characteristic for our experimental setup, $M = 6 \times 10^{-4}$ Nm/s) this apparently symmetric picture breaks down, and the in-phase synchronization is the one that is stable. Anti-phase synchronization is unlikely to be observed; it will appear only in the case when the two metronomes are started exactly in anti-phases ($\theta_2(0) = -\theta_1(0)$).

In view of these results, one can understand why only the stable in-phase synchronized dynamics was observed in our experiments. The results also emphasize the importance of using realistic model parameters in order to reproduce the observed dynamics.

7 Simulation results for several metronomes

Using the model defined in Section 4, our aim here is to theoretically understand the experimentally obtained trends. The equations of motion (9) and (10) were numerically integrated using a velocity Verlet-type algorithm as the integration method. A time-step of $dt = 0.01$ s was chosen. First, we intended to explain the experimental results presented in Figure 4. Seven metronomes with the same ω_i natural frequencies as the experimentally measured ones were considered, and the time-evolution of the Kuramoto order parameter was computed. Results obtained for different ω_0 frequency values are presented in the top panel of Figure 8. For the sake of better statistics we averaged the results of 100 simulations.

The obtained results are in good agreement with the experimental results presented in Figure 4.

Following our experiments, we have also studied the time-evolution of the order parameter for different

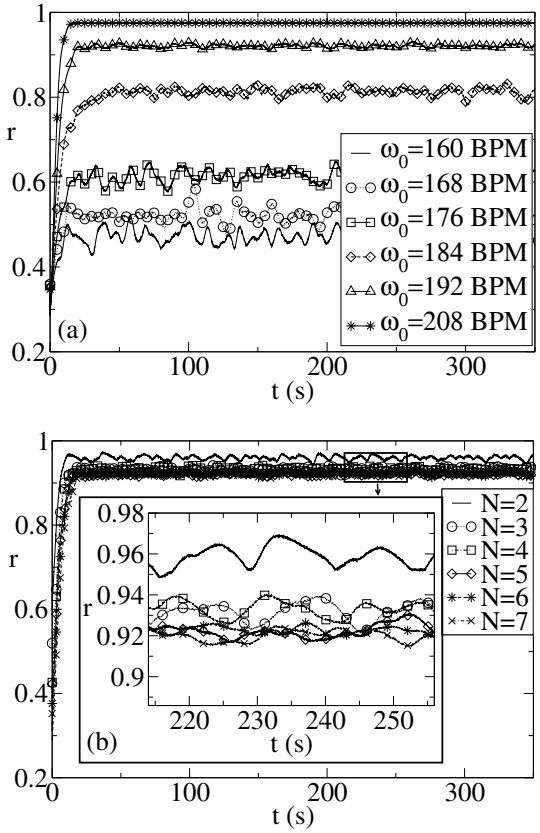

Fig. 8. Simulation results for the time-evolution of the Kuramoto order-parameter. (a) Results for the same natural frequencies as the ones used in the experiments. (b) Results for the same number of pendulums, and nominal beat frequency ($\omega_0 = 192$ BPM) as the ones used in the experiments. For both graphs, the presented results are an average over 100 independent simulations. The corresponding experimental results are presented in Figure 4.

numbers of pendulums, setting the same $\omega_0 = 192$ BPM natural frequency as in the experiments. Again, we averaged the results for 100 independent simulations. The obtained trend is sketched on the bottom panel of Figure 8.

The trend of the simulation results is in agreement with the experimental ones: increasing the number of metronomes results in a decrease in the observed synchronization level. In simulations, however, this decrease is not as evident as in the experiments. The reason for this could be the oversimplified manner in which we have handled the differences between the metronomes. In our model, the only difference between the metronomes are in the $L_2^{(i)}$ values (the distance of the movable weight from the horizontal suspension axes, see Fig. 2). In our simulations, the non-zero spread of these values is the sole source of the σ standard deviation for the frequencies ω_i. However, in reality many other parameters of the metronomes are different, leading to more different model parameters in their equations of motion. As a result of this, a more pronounced variation in the synchronization level is expectable.

In spite of the above discussed discrepancy, the simulation results suggest that our model with realistic model

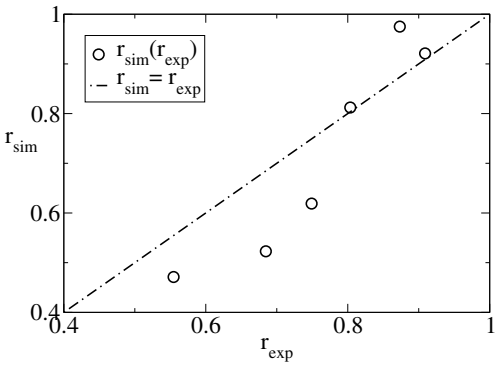

Fig. 9. Comparison between the simulated and experimentally obtained equilibrium synchronization level. Circles represent the results obtained for the ω_0 frequencies shown in Table 1. The straight dashed line indicates the optimal $r_{sim} = r_{exp}$ limit.

parameters works well for describing the dynamics of the coupled metronome system. In order to illustrate the effectiveness of our approach more quantitatively, we have plotted the simulated equilibrium synchronization level, r_{sim}, as a function of the experimentally determined value, r_{exp}, for the case of $N = 7$ metronomes. The plot from Figure 9 suggest that there is a satisfactory correlation.

Thus, one can investigate several interesting cases through simulations that are not feasible experimentally. Many interesting questions can be formulated this way. Here, we focus however only on clarifying the problems that we have investigated experimentally, namely the influence of the number of oscillators and the chosen natural frequency on the observed synchronization level.

Computer simulations will allow us to consider a higher number of metronomes and will also allow for a continuous variation of the metronomes' natural frequencies. Particularly, we are interested in clarifying whether, in the thermodynamic limit ($N \to \infty$), there is a clear $\omega_0 = \omega_c$ frequency threshold below which there is no synchronization in a system with fixed standard deviation (σ) of the metronomes' frequencies. Also, we would like to show that the reason for not obtaining a complete synchronization ($r = 1$) of the metronomes is the finite value of σ.

Considering a normal distribution of metronomes' natural frequency ω_i with a fixed standard deviation around the mean value of the standard deviations presented in Table 1 ($\sigma = 8 \times 10^{-7}$ BPM), we first studied how the Kuramoto order parameter, r, varies as a function of ω_0. Results obtained for a wide range of the number of metronomes, N, are plotted in the top panel of Figure 10.

The results plotted in Figure 10 suggest that, in the $N \to \infty$ limit, a clear phase-transition like phenomenom emerges. Around the value of $\omega_c = 185$ BPM the order parameter exhibits a sharp variation, which becomes sharper and sharper as the number of metronomes is increased. This is a clear sign of phase-transition like behavior.

Plotting the standard deviation of the order parameter values obtained from different experiments, we get a characteristic peak around the $\omega_c = 185$ BPM value. As is expected for a phase-transition-like phenomenon this

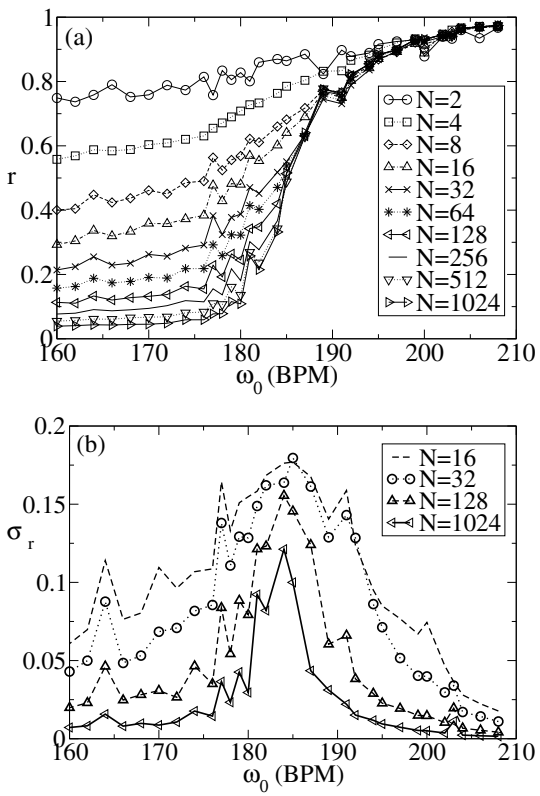

Fig. 10. Simulation results for the Kuramoto order parameter (a) and its standard deviation, σ_r, for the 100 computational experiments (b) as a function of the ω_0 frequency. Different curves are for different numbers of metronomes as indicated in the legends. In each case, the standard deviation of the metronomes' natural frequency ω_i is fixed as close as possible to $\sigma = 8 \times 10^{-7}$ BPM.

peak narrows as the number of metronomes on the disk increases.

Our next aim is to prove that the reason for not reaching the $r = 1$ complete synchronization is the finite standard deviation of the metronomes' natural frequencies. Simulations with up to 64 identical metronomes with $\omega_0 = 192$ BPM were considered, and the $r(t)$ dynamics of the Kuramoto order parameter was investigated. Results for different numbers of metronomes are plotted in Figure 11. From these graphs one can readily observe that in each case the completely synchronized state emerged. This proves that the lack of complete synchronization is due to the finite spread in the metronomes' natural frequencies. From this simulation we have also learned that variations of the equilibrium order parameter value as a function of N is also due to the finite σ value.

8 Conclusions

The dynamics of a system composed of coupled metronomes was investigated both by simple experiments and computer simulations. We were interested in finding the conditions for the emergence of synchronization.

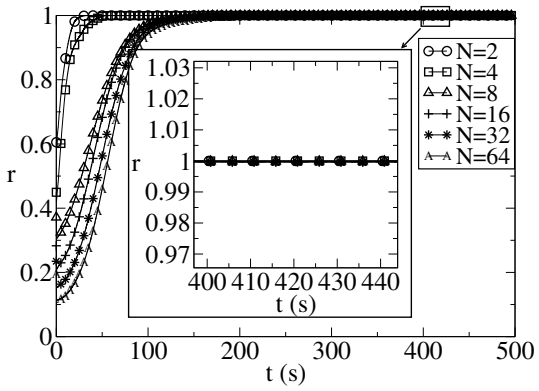

Fig. 11. Simulation results for identical metronomes. The time evolution of the order parameter for various numbers of metronomes, ranging from 2 to 64, is plotted ($\omega_0 = 192$ BPM).

Contrarily to many previous studies, here the problem was analyzed not from the viewpoint of dynamical systems, but from the viewpoint of collective behavior and emerging synchronization.

The experiments suggest that there is a limiting natural frequency of the metronomes below which spontaneous synchronization is not possible. By increasing the frequency above this limit, partial synchronization will emerge. The obtained synchronization level increases monotonically as the natural frequency of the oscillators increases. The experiments also suggest that increasing the number of metronomes in the system leads to a decrease of the observed synchronization level.

In order to better understand the dynamics of the system a realistic model was built. We have shown that damping due to friction forces and the presence of driving are both important in order to understand the emerging synchronization. The parameters of the model were fixed in agreement with the experimental conditions and the equations of motion were integrated numerically. The model proved to be successful in describing the experimental results, and reproduced the experimentally observed trends. The model allowed a fine verification of our findings regarding the conditions under which spontaneous synchronization emerges and the trends in the observed synchronization level. Computer simulations suggested that, for an ensemble of metronomes with a fixed standard deviation of their natural frequencies, the order parameter increases as a function of the metronomes' average frequency, ω_0. The model also suggests that this increase happens sharply for large ensembles, closely resembling a phase-transition like phenomenon. With the help of the simulations we have also shown that the reason behind an incomplete synchronization ($r = 1$) is the finite spread of the metronomes' natural frequencies ($\sigma \neq 0$).

The successes of the discussed model opens the way for many further studies regarding the dynamics of this simple system. Indeed, many other interesting questions can be formulated regarding the influence of the metronome and rotating platform parameters on the obtained synchronization level and the observed trends. Also, one can study systems where the metronomes or groups of metronomes are fixed to different natural frequencies, or where there is an external driving force acting on the system. The discussed model has the advantage that the equations of motion are easily integrable and the model parameters are realistic, with a direct connection to the parameters of an experimentally realizable system.

Finally, we hope that the novel experimental setup and the results presented here will help in clarifying some aspects for one of the oldest problems in physics, namely the spontaneous synchronization of coupled pendulum clocks. Although several similar problems have been considered in previous studies, we have shown that there are still many fascinating aspects that one can investigate in this simple mechanical system.

Work supported by the Romanian IDEAS research Grant PN-II-ID-PCE-2011-3-0348. The work of B.Sz. is supported by the POSDRU/107/1.5/S/76841 PhD fellowship. B. Ty. acknowledges the support of Collegium Talentum Hungary. We thank E. Kaptalan from SC Rulmenti Suedia for constructing the rotating platform.

References

1. S. Strogatz, *Sync: The Emerging Science of Spontaneous Order* (Hyperion, New York, 2003)
2. S. Strogatz, Physica D **226**, 181 (2000)
3. A. Pikovsky, M. Rosenblum, J. Kurths, *Synchronization: A Universal Concept in Nonlinear Science* (Cambridge University Press, Cambridge, 2002)
4. C. Huygens, in *Oeuvres Complètes de Christian Huygens*, edited by M. Nijhoff (Societe Hollandaise des Sciences, The Hague, 1893), Vol. 5, p. 243 (a letter to his father, dated 26 Feb. 1665)
5. M. Bennet, M.F. Schatz, H. Rockwood, K. Wiesenfeld, Proc. Roy. Soc. London A **458**, 563 (2002)
6. R. Dilao, Chaos **19**, 023118 (2009)
7. M. Kumon, R. Washizaki, J. Sato, R.K.I. Mizumoto, Z. Iwai, in *Proceedings of the 15th IFAC World Congress, Barcelona, 2002*
8. A.L. Fradkov, B. Andrievsky, Int. J. Non-linear Mech. **42**, 895 (2007)
9. K. Czolczynski, P. Perlikowski, A. Stefanski, T. Kapitaniak, Int. J. Bifur. Chaos **21**, 2047 (2011)
10. K. Czolczynski, P. Perlikowski, A. Stefanski, T. Kapitaniak, Physica A **388**, 5013 (2009)
11. J. Pantaleone, Am. J. Phys. **70**, 992 (2002)
12. B. van der Pol, Philos. Mag. **3**, 64 (1927)
13. Y. Kuramoto, I. Nishikawa, J. Stat. Phys. **49**, 569 (1987)
14. H. Ulrichs, A. Mann, U. Parlitz, Chaos **19**, 043120 (2009)
15. M. Kapitaniak, K. Czolczynski, P. Perlikowski, A. Stefanski, T. Kapitaniak, Phys. Rep. **517**, 1 (2012)
16. Wikipedia, *Metronom* (2012 (accessed July 23, 2012)), https://en.wikipedia.org/wiki/Metronome
17. Wikipedia, *Minicom* (2012 (accessed January 14, 2012)), https://en.wikipedia.org/wiki/Minicom